ACS OMEGA

http://pubs.acs.org/journal/acsodf

Article

Temperature and pH Dual Responsive Nanogels of Modified Sodium Alginate and NIPAM for Berberine Loading and Release

Shuhua Chang, Dawei Qin,* Rongjun Yan, Mengli Zhang,* Binglin Sui, Hui Xu, Zhaomin Zheng, Xiaoli Hou, Yonggang Wang, and Chenggang Qi

Cite This: *ACS Omega* 2021, 6, 1119−1128

Read Online

ACCESS | Metrics & More | Article Recommendations

ABSTRACT: pH- and temperature-sensitive nanogels (NGs) were prepared from sodium alginate (SA) and *N*-isopropylacrylamide (NIPAM), as the sensitivity at pH 5.5 and 31 °C. SA was pH-modified with glutamic acid (Glu) and ethylenediamine (EDA). The products Glu-SA (Glu-modified SA) and EGSA (EDA- and Glu-modified SA) were characterized by ninhydrin color reaction, infrared spectroscopy, and zeta potential, and the best reactant ratio was selected. Moreover, temperature-sensitive, pH-sensitive EGSA-NGs possessing a semi-interpenetrating network structure were prepared by radical polymerization using *N*-isopropylacrylamide. The morphology of EGSA-NGs was characterized by transmission electron microscopy (TEM), scanning electron microscopy (SEM), and atomic force microscopy (AFM). The cytotoxicity test shows the low cytotoxicity and high biocompatibility of the NGs. The newly prepared NGs were also subjected to pH-sensitive temperature-sensitive in vitro drug-loading and drug-release experiments. The pH-sensitive and temperature-sensitive experiments showed that the particle size of EGSA-NGs was reduced at pH 5.5 and above 31 °C. The drug-loading and drug-release experiments also confirmed this finding, indicating that the newly synthesized NGs could release the drug according to the environmental changes. Therefore, the material has potential application value in solid tumor targeted therapy.

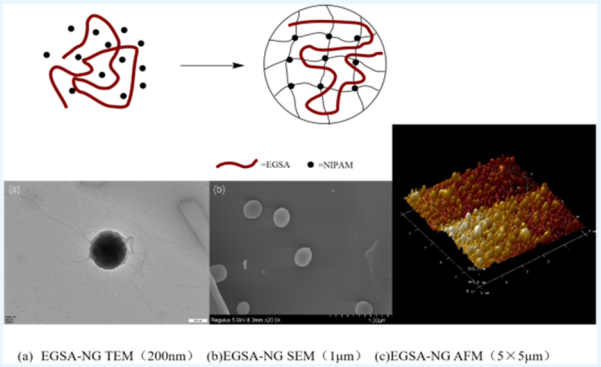

(a) EGSA-NG TEM（200nm） (b)EGSA-NG SEM（1μm） (c)EGSA-NG AFM（5×5μm）

INTRODUCTION

Nanoparticles (NPs) possess many properties not found in conventionally sized materials due to their unique size and specific surface area. NPs are widely used in biology, medicine, agriculture, and other industries.[1−4] Nanogels (NGs), a special type of NP, generally referred to macromolecular polymer particles from 10 to 500 nm, are swellable nanonetworks composed of hydrophilic or amphiphilic polymer chains. NG is an excellent promising drug delivery carrier, which has high loading capacity, high stability, and high ability to respond to external environmental stimuli, such as ionic strength, pH, and temperature as well as other common nanomedicines.[5−8] The carrier is unique and unprecedented.

Moreover, pH-sensitive NGs can be slowly released in the general environment, while they can be rapidly released in the target environment. Therefore, they have been considered as promising anticancer drug carriers. Yu et al. have used chitosan and ovalbumin to prepare stable NGs, which are synthesized by the green method.[9] The prepared NG consists of ovalbumin nanospheres containing some chitosan chains interspersed in the NG structure, with the remainder being shells. The 100 nm-sized NG is pH-sensitive, and its hydrodynamic radius is constant over a pH range of 4.3−5, which is increased over a pH range of 5−5.3 and strongly increased within the pH range of 5.3−5.8. They have also reported changes in hydrophobicity/hydrophilicity relative to pH. NGs are hydrophilic at neutral and acidic pH and hydrophobic at alkaline pH. Therefore, NGs can be used for drug delivery due to their pH responsiveness.

In recent years, the rapid development of nanocarriers as delivery systems has greatly contributed to the treatment of cancer.[10] Many NP-based therapeutics have been approved for clinical use in solid tumors, such as Doxil (pegylated liposomal doxorubicin)[11] and Abraxane (Paclitaxel bond with albumin NPs).[12−14] Cancer cells have unique biological phenomena. This phenomenon is known as the enhanced permeability and retention (EPR) effect.[15] Many vascular endothelial growth factors (VEGPs) are secreted due to the rapid growth of cancer cells, leading to rapid growth of blood vessels in solid tumors,

Received: August 17, 2020
Accepted: November 20, 2020
Published: January 4, 2021

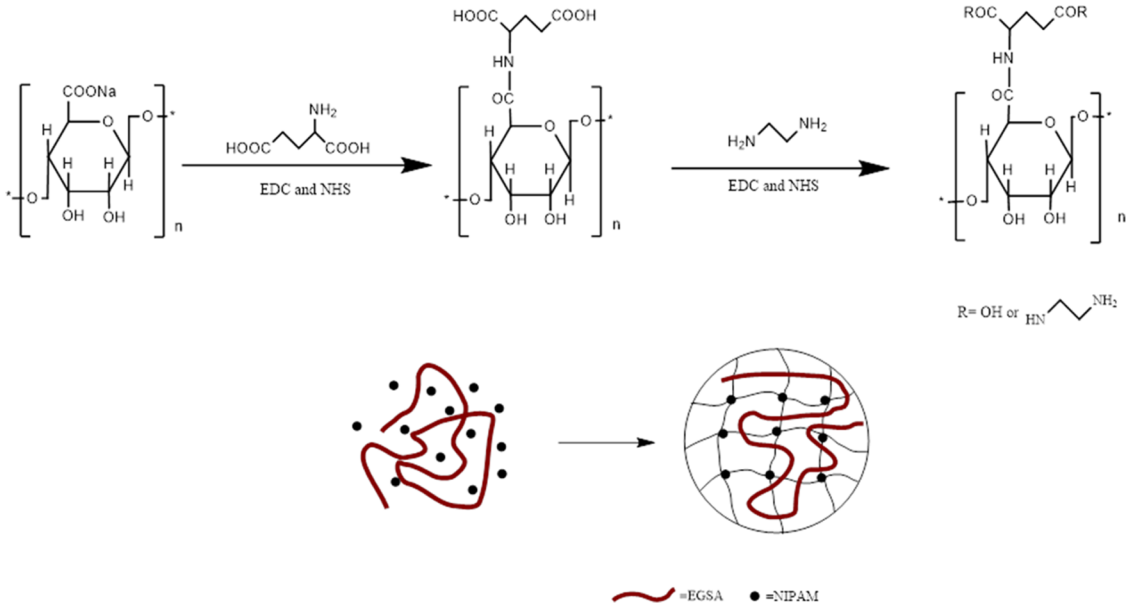

Figure 1. Preparation process of EGSA-NGs.

which results in the rearrangement and transportation of rapidly growing vascular cells. The gap between cells is large, lacking a smooth muscle layer and lymphatic reflux.[16−18] Such properties of solid tumor blood vessels render NPs of a certain size to enter through blood vessels and remain in the vicinity of cancer cell tissue.

To achieve the goal of drug release, an obtainable, biocompatible, and modifiable material must be used as the raw material of our nanogels. SA is an easily obtainable polysaccharide with abundant cationic groups, which can be found in some seaweed. With the natural pH sensitivity, what we should do is changing its charge distribution to change its pH sensitivity by modification with Glu and EDA. The pH of the modified SA can be adjusted to an available range to qualify as a drug release material in the human body. Then with temperature-sensitive NIPAM semi-interpenetrating cross-linking, we have obtained nanogels that can respond simultaneously to the temperature and pH of the internal environment of humans. The process is shown in Figure 1.

In the past two decades, there have been reports that berberine can induce apoptosis of solid tumor cancer cells. In the existing reports, berberine can inhibit the growth and proliferation of colon cancer, esophageal cancer, lung cancer, and liver cancer cells,[19−22] which shows its potential anticancer ability. However, berberine hydrochloride has low biocompatibility due to its poor water solubility, and a higher dosage is needed to achieve the desired effect. In order to improve the bioavailability of berberine hydrochloride, researchers have designed many carriers for it to achieve the purpose of treatment. Grebinyk and his research group designed a drug delivery system that combines berberine with a DNA carrier to treat leukemia.[23]

In the present study, we aimed to synthesize a pH- and temperature-sensitive nanogel using biocompatible materials. The optimum ratio of reactants was studied, and the regulatory mechanism of pH sensitivity was explored. In addition, we tested the release capacity of the newly synthesized nanogels in a simulated solid tumor environment.

RESULTS AND DISCUSSION

Fourier Transform Infrared (FTIR) Spectrometry. In Figure 2, in the IR spectrum of glutamic acid-sodium alginate

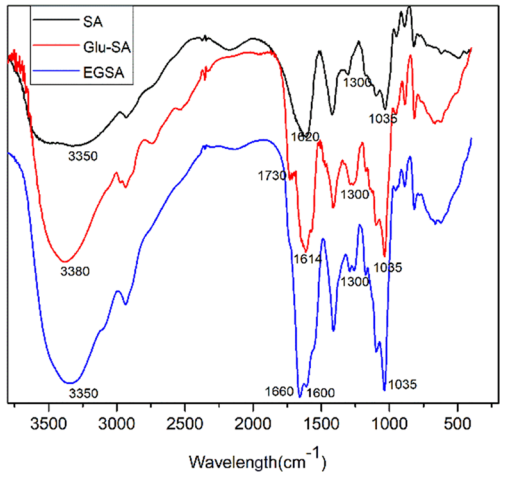

Figure 2. FTIR spectra of SA, Glu-SA, and EGSA.

(Glu-SA), there was a new absorption peak at 1730 cm^{-1}, which was the peak of the amide I band, and the peak at 1614 cm^{-1} became strong, which was the overlapped peak of the amide II band. The amide III band peak also became apparent at 1300 cm^{-1}, indicating that an amide bond was formed in Glu-SA. The absorption peak at 1090 cm^{-1} was a characteristic peak of the pyranose ring, and there was no change in Glu-SA, indicating that the graft had no effect on the pyranose ring. The characteristic peaks in the Glu-SA spectrum, such as the amide I, II, and III bands, were also present in the EGSA spectrum, and the characteristic peak of the pyranose ring at 1035 cm^{-1} was also present. The most obvious change was that the peak of the amide I band was shifted to 1660 cm^{-1}, and the absorbance was also greatly enhanced. Therefore, we speculated that the content of the amide bond in the molecule was greatly increased. The shape of the −OH and −NH− stretching vibration peaks at the position of 3350 cm^{-1} was

https://dx.doi.org/10.1021/acsomega.0c03965
ACS Omega 2021, 6, 1119−1128

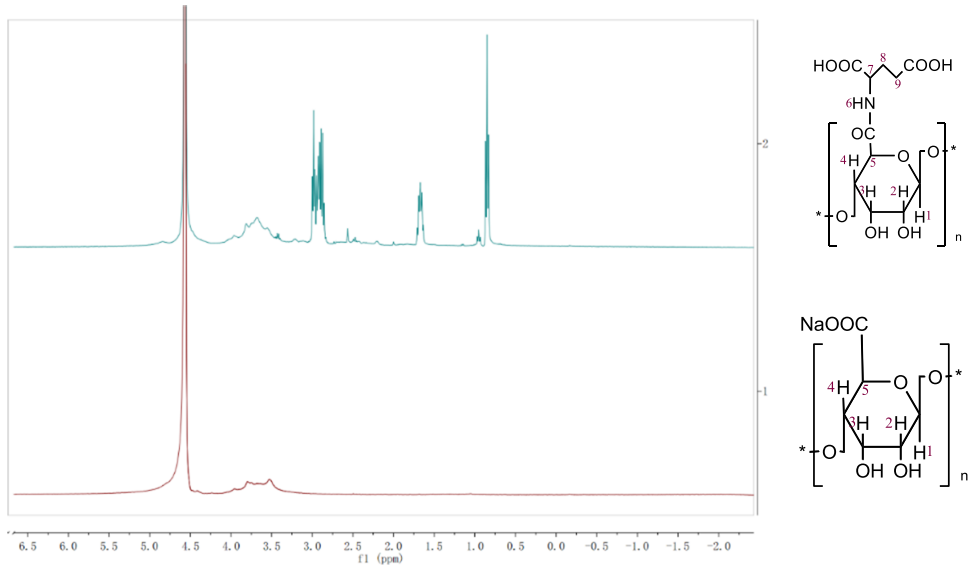

Figure 3. ^{1}H NMR spectra of SA and Glu-SA.

slightly twisted to the right, which might be attributed to the redistribution of charge on the carboxyl group and the amino group. Collectively, both Glu-SA and EGSA were successfully synthesized.

^{1}H Nuclear Magnetic Resonance (NMR). Since SA and Glu-SA are macromolecules, we could identify the product by integrating the peak area. Therefore, it was necessary to combine the characteristic peaks appearing in the IR spectrum to determine whether a reaction occurred.

SA was characterized using ^{1}H NMR (D_2O, 400 MHz, δ ppm), Glu-SA was characterized using ^{1}H NMR (D_2O, 400 MHz, δ ppm). Through the comparison of the NMR spectra of SA and Glu-SA in Figure 3, we found that the NMR spectrum of Glu-SA had new peaks at 0.8, 1.6, and 3.0 ppm. According to the structure of our target product, the peak at 1.0 ppm should belong to H8 and H9 hydrocarbyl hydrogens. H7 would move to a higher chemical shift due to the influence of adjacent amino groups. Therefore, the peak at 1.6 ppm belonged to H7. The peak at 3.0 ppm was a characteristic peak of H6 on the amino group. A shielding effect was exerted on the H of the carboxyl group because of the use of the solvent D_2O. Therefore, there was no peak belonging to the carboxyl group in the spectrum.

Degree of Substitution (DS). The DS was calculated using eq 1

$$\mathrm{DS}\ (\%) = \frac{w_G}{w_0} \times 100 \tag{1}$$

where w_G and w_0 are the masses of Glu and Glu-SA in the solution, respectively.

The curve of relationship between the amount of Glu and DS was obtained. Figure 4 shows that as the amount of Glu added was increased, the DS of the product was also gradually increased. When the input amount of Glu reached 1.280 g, the increase of the grafting rate began to slow. When the input amount of Glu reached 2.544 g, the DS reached 40.61%, which could be regarded as the expected DS. Although the DS was slightly increased under $n_{SA\ unit}$:n_{Glu} = 1:3, it was necessary to add more Glu (about 1.3 g). In order to save raw materials, we selected $n_{SA\ unit}$:n_{Glu} = 1:2 as the best reactant ratio for the grafting reaction.

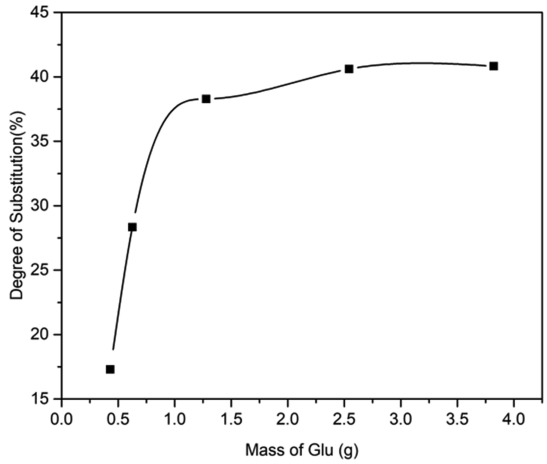

Figure 4. Effect of the Glu amount on DS.

Zeta Potential. The zeta potentials of five EGSA products at different pH values were detected (Figure 5). We connected

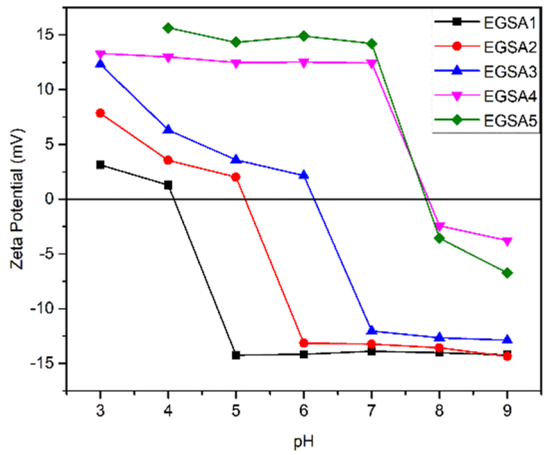

Figure 5. Zeta potential of EGSA with different reactant ratios (EGSA1, 2, 3, 4, and 5 were the mass ratios between Glu-SA and EDA at 10:1, 10:2, 10:3, 10:4, and 10:5, respectively).

https://dx.doi.org/10.1021/acsomega.0c03965
ACS Omega 2021, 6, 1119−1128

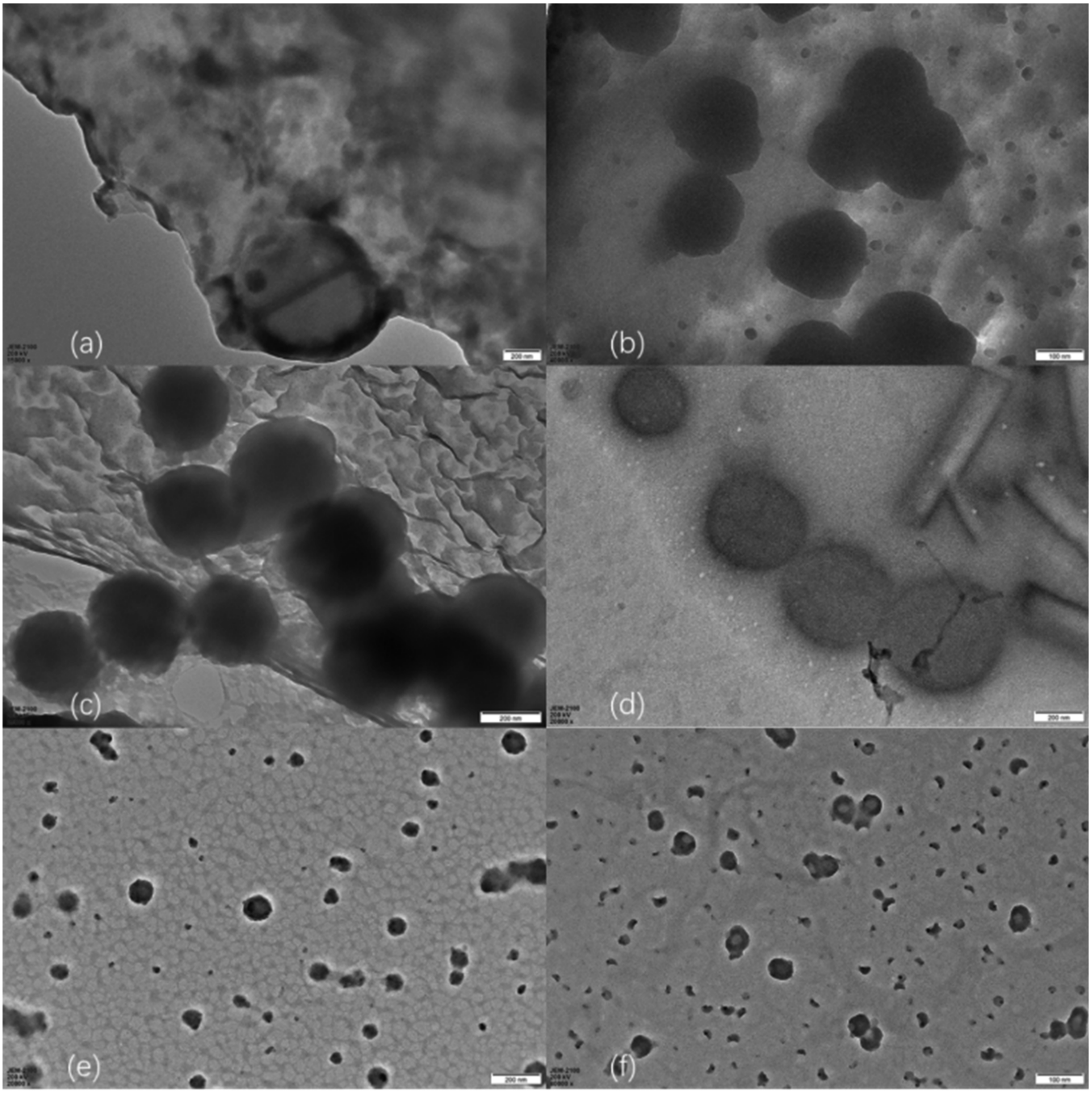

Figure 6. TEM images. (a) EGSA:NIPAM = 1:0 scale bar: 200 nm; (b) EGSA:NIPAM = 2:1 scale bar:100 nm; (c) EGSA:NIPAM = 1:1 scale bar:200 nm; (d) EGSA:NIPAM = 1:2 scale bar: 200 nm; (e) EGSA:NIPAM = 1:3 scale bar: 200 nm; (f) EGSA: NIPAM = 0:1 scale bar: 200 nm.

the points at corresponding pH values together when a zeta potential of zero was regarded as the isoelectric point (pI) of the product. Figure 5 illustrates that as the amount of ethylenediamine (EDA) was increased, the pI of EGSA was gradually increased from the lowest 4.2 to the highest 7.8, which covered most of the pH environment in the human body. This finding also showed that the ratio of Glu-SA to EDA could be varied depending on the release environment to change its corresponding pH sensitivity. Based on the characteristic environment in solid tumor cells, we selected EGSA1 ($m_{\text{Glu-SA}}$:m_{EDA} = 10:1), which was sensitive to the acidic environment, as the reactant material for the next step.

Electron Microscopic Characterization. Figure 6 shows that the particle size of NGs was increased accordingly when the amount of EGSA was increased. Figure 6a exhibits that when there was no *N*-isopropylacrylamide (NIPAM) participation in the reaction, the hydrogel could not be formed. Figure 6b,c shows that although NGs with uniform shape and good particle dispersion were prepared, the NGs were encapsulated in the unreacted EGSA, which might affect the properties of EGSA-NGs. This finding indicated that the treatment in our preparation process could not remove excess EGSA. Therefore, the ratios in panels (b) and (c) were not the best ratios that we expected. For Figure 6d, uniformly stable NGs were formed with sizes of about 400 nm. The crystalline

https://dx.doi.org/10.1021/acsomega.0c03965
ACS Omega 2021, 6, 1119−1128

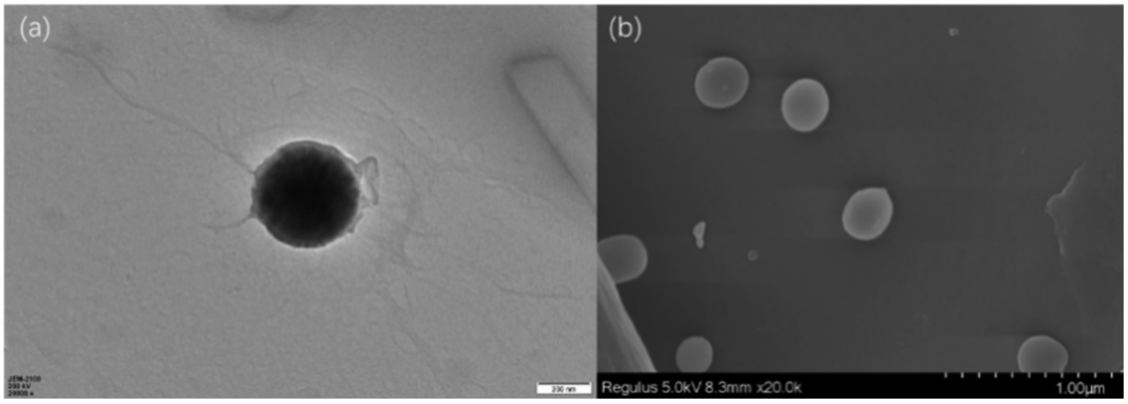

Figure 7. 20,000× electron micrographs of NGs. (a) TEM image, scale bar: 200 nm; (b) SEM image, scale bar: 1 μm.

compound on the right side of the visual field might be lyoprotectant mannitol crystals, which could be removed by dialysis. Figure 6e reveals that it was also possible to form regularly shaped NGs with a particle size below 100 nm and a larger specific surface area, while the particle size distribution was not uniform enough. The structure was defective, which was manifested in the damaged spherical particles. This might be attributed to the insufficient mechanical strength of the high content of PNIPAM, which might not be able to withstand external forces during the dispersion process. In Figure 6f, this phenomenon became more obvious. There were many broken NGs in the field of view, indicating that the NGs formed by adding only NIPAM had very poor physical strength. Most NIPAM NGs would be broken after going through stirring and ultrasonic energy during the redispersion process.

In summary, the shape of the NGs formed under the ratio in Figure 6d was intact and uniform, the particle size distribution was good, and there were no impurities that could not be removed.

Figure 7 shows that with an EGSA:NIPAM ratio of 1:2, the shape of the NGs was uniform, and the surface was smooth, showing no obvious protrusion or sinking, which indicated that it could be transported in the blood with less resistance.

Figure 8 exhibits that the particle size distribution of the NGs was relatively uniform, and it was mostly distributed between 350 and 500 nm. NGs exhibited a regular spherical shape, where slight agglomeration might be attributed to higher sample concentrations.

The size distribution of particles was measured and recorded three times (Figure 9). The particle sizes of the three records were 433.6, 453.2, and 467.6 nm. The PdI values were all less than 0.3, indicating that the size distribution of hydrogel particles was uniform. The average value of the three records was taken as the average particle size of EGSA-NGs, which met the requirement for drug loading and delivery.

Environmental Sensitivity. Finally, the transmittance curve of the EGSA-NGs was obtained (Figure 10). The corresponding pH at the highest transmittance was the responsive pH value of EGSA-NGs. When the pH was 3, the carboxyl groups in the molecules were almost uncharged, and a small amount of the amino groups was positively charged. However, since the amount of protonated amino groups was still relatively small compared with the entire ion, the solution was clear. As the pH was gradually increased, the protonated amino group gradually lost its proton recovery to an uncharged state. When the pH reached 5−5.5, it was the pI of the NGs.

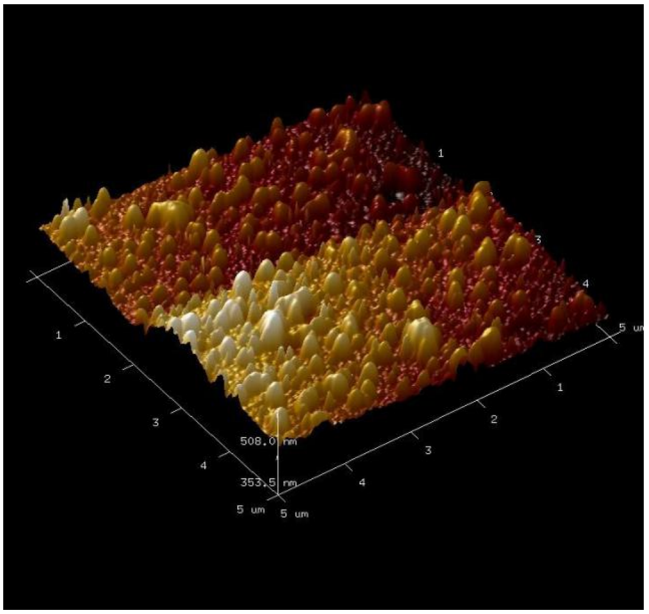

Figure 8. AFM image for the undulation of the surface of the slide carrying NGs (5 μm × 5 μm).

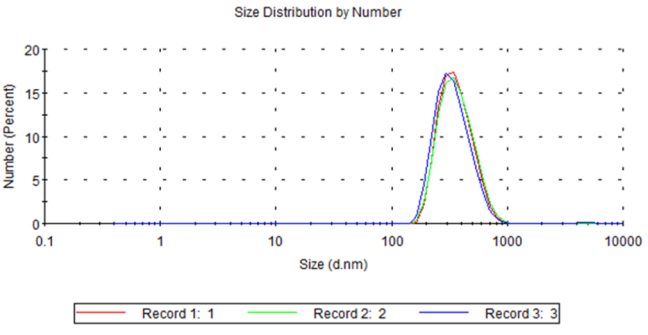

Figure 9. Particle size distribution image.

There was no electrostatic repulsion between the molecules, the particle size of the hydrogel molecules was minimized, and the transmittance of the solution was also the highest. As the pH was further increased, the carboxyl groups in the molecule began to deprotonate, the charge of the entire molecule gradually changed from positive to negative, the intermolecular repulsion was increased, and the solution began to be cloudy from turbidity. Moreover, when the pH reached 7, the

https://dx.doi.org/10.1021/acsomega.0c03965
ACS Omega 2021, 6, 1119−1128

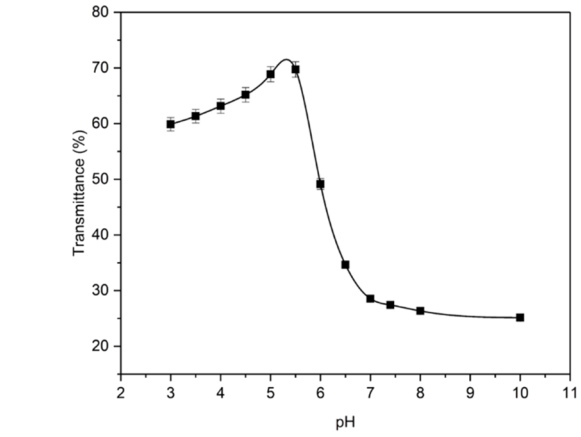

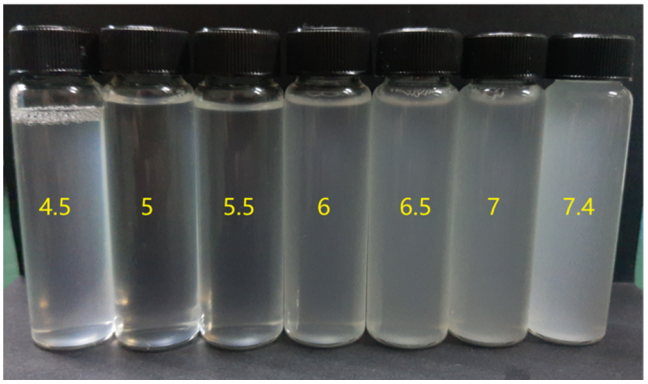

Figure 10. pH sensitivity curve (top) and colorimetric experiment (bottom).

deprotonation was basically completed. At this time, since the content of the carboxyl groups in the solution was much higher than that of amino groups, the transmittance of the solution under the alkaline conditions was lower than that under the acidic conditions.

The curve of transmittance with temperature was obtained (Figure 11), and the corresponding temperature of EGSA-NGs was obtained when the transmittance was rapidly decreased. The transmittance of the NG solution was decreased with the increase of temperature. When the temperature was higher than 30 °C, the light transmittance was rapidly decreased. When the temperature was close to the LCST of the NGs, the phase transformation occurred. When the temperature exceeded 31 °C, all molecules completed the phase transition, and the molecules changed from the hydrophilic phase to the hydrophobic phase. Due to the repulsive force of the water molecules in the solution, the NGs became smaller in size, and the solution appeared to be opaque. After 33 °C, the transmittance curve tended to be flat. We could get 31−33 °C as the responsive temperature interval of EGSA-NGs. The narrow interval and rapid response indicated that EGSA-NGs had good thermal sensitivity and could respond to the human body temperature environment after entering the human body, thereby smoothly releasing the drug.

Cytotoxicity of EGSA-NGs. The cell viabilities at the treatment of different concentrations of EGSA-NGs are shown in Figure 12. All the cell viabilities are higher than 95% with the treatment of EGSA-NGs, which shows that the material has relatively lower cytotoxicity. Also, Figure 12 shows that its cytotoxicity does not increase with concentration of EGSA-

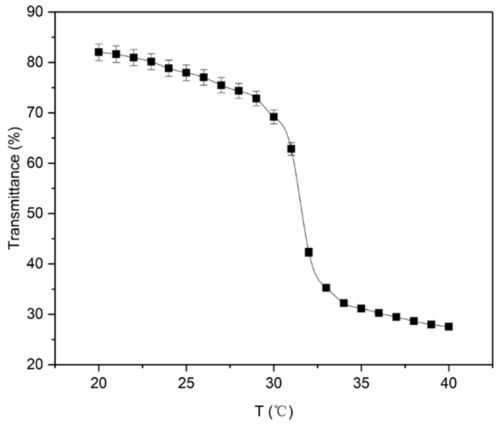

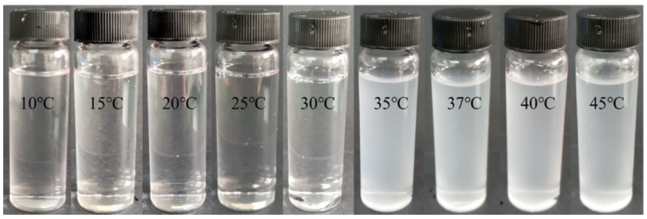

Figure 11. Thermal sensitivity curve (top) and colorimetric experiment (bottom).

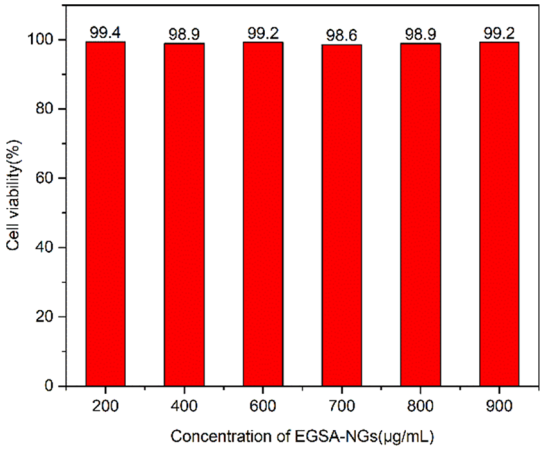

Figure 12. Cell viability of HFF cells with the treatment of EGSA-NGs.

NGs. In summary, EGSA-NG is a safe and low-toxic material, which shows enormous potential as drug carriers.

Drug Loading and Release Capacity. The drug loading ratio was calculated using eq 2

$$\mathrm{DS}\ (\%) = \frac{w_1 - w_2}{w_0} \times 100 \tag{2}$$

where w_1 is the mass of berberine hydrochloride added during drug loading, w_2 is the mass of unloaded berberine hydrochloride, and w_0 is the mass of the finally obtained drug-loaded EGSA-NGs.

The drug loading rate was 28.02% from the calculation formula of the drug loading rate, indicating that 1 g of drug-loaded EGSA-NGs contained 0.2802 g of berberine.

The drug release curves are shown in Figure 13. The cumulative release of the drug was increased with time. The release of the drug was rapidly increased in the first 5 h at the

https://dx.doi.org/10.1021/acsomega.0c03965
ACS Omega 2021, 6, 1119−1128

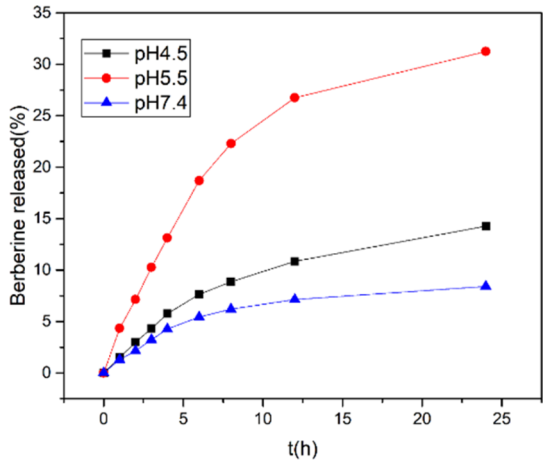

Figure 13. Cumulative release curves of berberine at three different pH values.

three pH values. After 5 h, the drug release began to slow down and grew slowly after 10 h. At the three pH values, the cumulative release was the highest within 24 h at pH 5.5, reaching 31.25%. Second, under the condition of pH 4.5, the cumulative drug release was 14.28% within 24 h, the release amount was the least when pH = 7.4, and only 8.41% of the drug was released within 24 h. The differences in the release rates at the three different pH values indicated that NGs responded most strongly at pH 5.5.

CONCLUSIONS

The EGSA-NG material was prepared by modifying SA with Glu and EDA, which was characterized by IR, NMR, zeta potential, transmission electron microscopy (TEM), scanning electron microscopy (SEM), atomic force microscopy (AFM), and so on. The EGSA-NG material had dual sensitivity to pH and temperature. In a characteristic pH environment, the NGs can load drugs to achieve intelligent drug release. With its pH responsiveness, the pH value of the non-pI could load the drug molecules. When the pH of the environment was equal to the pI of the NGs, the interaction between the cross-linked networks was weakened, and the NGs collapsed to achieve rapid drug release. Also, the shown low toxicity of the NGs to HFF cells confirms adequate safety of EGSA-NGs. The pH values of lysosomes and endosomes in solid tumor cells are 4.5 and 5.5, respectively, which are approximate to the pI of EGSA-NGs. Therefore, the material has potential application value in solid tumor targeted therapy.

MATERIALS AND METHODS

Materials. SA was purchased from Sinopharm Chemical Regent Co., Ltd. (Shanghai, China). 1-(3-Dimethylaminopropyl)-3-ethylcarbodiimide hydrochloride (EDC·HCl) and *N*-hydroxysuccinimide (NHS) were obtained from Shanghai Macklin Biochemical Co., Ltd. (Shanghai, China). Glu was supplied by Shanghai Aladdin Bio-Chem Technology Co., Ltd. (Shanghai, China). NIPAM was provided by Sann Chemical Technology Co., Ltd. (Shanghai, China). *N*,*N*′-Methylenebisacrylamide (MBA) was purchased from Tianjin Kermel Chemical Reagent Co., Ltd. (Tianjin, China). Ammonium persulfate (APS) was obtained from Tianjin Damao Chemical Reagent Factory (Tianjin, China). Berberine hydrochloride was purchased from Qilu Pharmaceutical Co., Ltd. (Jinan, China).

Synthesis of pH-Sensitive EGSA. Briefly, 2.012 g of SA was accurately weighed and dissolved in 200 mL of distilled water, and the mixture was stirred at room temperature until a uniform and stable SA solution was formed. The SA solution was activated by adding 4.998 g of EDC·HCl followed by stirring for 30 min. In addition, 2.009 g of NHS and different amounts ($n_{SA\ units}$:n_{Glu} = 3:1, 2:1, 1:1, 2:1, 3:1) of Glu were added into the abovementioned solution followed by stirring at room temperature for 24 h. The resultant solution was dialyzed in a 3500 Da dialysis bag for around 72 h. Afterward, the Glu-SA powder was obtained by freeze-drying for 12 h.

Subsequently, 0.200 g of Glu-SA was accurately weighed and dissolved in 20 mL of distilled water, and the mixture was stirred at room temperature until a uniform and stable Glu-SA solution was formed. The Glu-SA solution was activated by adding 0.520 g of EDC·HCl followed by stirring for 30 min. Next, 0.313 g of NHS and different amounts (0.020, 0.040, 0.060, 0.080, and 0.100 g) of EDA were added into the abovementioned solution followed by stirring at room temperature for 24 h. The resultant solution was dialyzed in a 3500 Da dialysis bag for around 72 h. Afterward, the pH-sensitive EGSA powder was obtained by freeze-drying for 12 h. The products were named EGSA1, EGSA2, EGSA3, EGSA4, and EGSA5.

The structures of Glu-SA and EGSA were characterized by FTIR (IRPrestige-21, Shimadzu, Japan).

Synthesis of Environmentally Responsive NGs. Briefly, 2.000 g of NIPAM was weighed and dissolved in 100 mL of distilled water. Afterward, 0.100 g of cross-linker MBA and different amounts (m_{EGSA}:m_{NIPAM} = 1:0, 2:1, 1:1, 1:2, 1:3, 0:1) of EGSA were added into the solution, and the resultant solution was stirred and dispersed under vacuum until a stable and uniform solution was formed. Subsequently, 0.020 g of APS was added as an initiator after the temperature of solution was increased to 60 °C. The mixture was reacted at the constant temperature (60 °C). The environmentally responsive NGs (EGSA-NGs powder) were obtained after 72 h of dialysis in a 5000 Da dialysis bag and 12 h of freeze-drying.

Degree of Substitution (DS). The DS was determined by ninhydrin coloration reaction and UV spectrophotometry. The concentration of amino groups in the solution was linearly and positively correlated with the UV absorbance at the corresponding wavelength. Briefly, accurately weighed Glu (0.0118, 0.0192, 0.0329, 0.0399, and 0.487 g) was added into five 100 mL volumetric flasks and brought to volume with distilled water. Glu standard solutions at concentrations of 1.18×10^{-4}, 1.92×10^{-4}, 3.29×10^{-4}, 3.99×10^{-4}, and 4.87×10^{-4} g/mL were prepared. Next, 2 mL of Glu standard solution at the abovementioned five concentrations was added into 50 mL colorimetric tubes. Then 1.5 mL of ninhydrin solution (2%) and 1 mL of phosphate buffer solution (pH = 6.7) were added followed by heating in a boiling water bath for 18 min, and then the solution was brought to volume with distilled water. The UV absorbance at 567 nm was recorded, and a Glu standard curve was established. In addition, 0.2 g of Glu-SA prepared with different molar mass ratios between SA units and Glu was weighed and dissolved in 50 mL of hydrochloric acid solution (2 M), which was heated under reflux at 95 ° C for 3 h, and the Glu-SA products were decomposed. The appropriate amount of 2 M NaOH solution was added to neutralize the hydrochloric acid in the solution, and the free

https://dx.doi.org/10.1021/acsomega.0c03965
ACS Omega 2021, 6, 1119−1128

Glu in the solution was developed by the above-described ninhydrin reaction. The absorbance of the solution at a wavelength of 567 nm after the coloration was determined using a UV spectrophotometer (TU-1900, Puxi, Shanghai), and the relative concentration of Glu was calculated from the obtained Glu standard curve.

Zeta Potential. The EGSA products were formulated into 0.5% solutions and stirred for 4 h until the products were uniformly dispersed. The pH of the EGSA solutions was adjusted to 3, 4, 5, 6, 7, 8, and 9, respectively. The zeta potentials of EGAS solutions were determined using a Zetasizer (ZS90, Malvern, UK) to screen the best reactant material ratio.

Characterization of EGSA-NGs. To screen the best material ratio, TEM was used to observe the morphology of the NGs. The EGSA-NG powder with different material ratios was dissolved in distilled water to prepare 0.1% EGSA-NG solutions. The copper grids (300 mesh) were dipped into the solutions and then dried in a vacuum drying oven at 80 °C for 10 h. Afterward, the samples on the copper grids were stained with 2% phosphotungstic acid. The samples were observed by TEM (JEM-2100, JEOL, Japan) after vacuum drying for 8 h.

For SEM characterization, the surface morphology of EGSA-NGs with the best reactant material ratio was observed. A small piece of conductive tap was pasted on the stage. The optimal NG product powder was smeared on the conductive tap. After conductive gold coating, the stage carrying the sample was observed by SEM (Regulus, Hitachi, Japan).

For AFM characterization, the particle size distribution of EGSA-NGs with the best reactant material ratio was roughly observed. The sample was dissolved in distilled water to formulate a 0.5% solution. The solution was dropped on the surface of a 0.5 × 0.5 cm^2 glass slide, which was vacuum-dried at 50 °C for 10 h to remove all the moisture of the sample.

The particle size of the above sample solution was detected using a Zetasizer.

Environmental Sensitivity. Both pH and thermal sensitivities were characterized through determining the transmittance variations.

For pH sensitivity determination, 0.200 g of EGSA-NG powder was dissolved in 200 mL of distilled water. The pH value of EGSA-NG solution was adjusted to 3, 3.5, 4, 4.5, 5, 5.5, 6, 6.5, 7, 7.4, 8, and 10 using 0.1 M HCl or 1 M NaOH solution. The transmittances of 12 types of EGSA-NG solutions with different pH values were detected using a UV spectrophotometer at a wavelength of 560 nm.

For thermal sensitivity determination, 0.010 g of EGSA-NG powder was dissolved in 10 mL of distilled water. The temperature of the solution was increased from 20 to 40 °C, with an increment of 1 °C, and the transmittance of the solution was detected using a UV spectrophotometer at a wavelength of 560 nm.

Similarly, the particle size of EGAS-NGs at different temperatures was detected using a Zetasizer.

Cytotoxicity Test. The cytotoxicity of EGSA-NGs was tested. Human foreskin fibroblasts (HFF) were chosen as the normal cell for the methyl thiazolyl tetrazolium (MTT) assay.

After the cell passage, 200 μL of cell culture fluid was transferred into 96-well plates, and the number of cells was observed and counted under the microscope (DX81, Olympus, Japan). By dilution, the number of cells reached 5000−10,000 per well. The cells were cultured in a CO_2 incubator for 24 h.

After that, the cells were treated with PBS solution and EGSA-NGs. The concentrations of EGSA-NGs were set to 200, 400, 600, 700, 800, and 900 μg/mL. After treatment for 48 h in a CO_2 incubator, MTT solution (5%) was added into the 96-well plates, and the cells were cultured for another 4 h in a CO_2 incubator. Finally, the medium was replaced by DMSO. After shaking in the dark for 10 min, the optical densities were measured by a microplate reader (DNM-9602, Perlong, Beijing) at 570 nm to calculate the cell viability using eq 3

$$\text{cell viability (\%)} = \left(1 - \frac{OD_1}{OD_0}\right) \times 100 \quad (3)$$

where OD_1 is the average optical densities after the treatment of EGSA-NGs and OD_0 is the average optical densities after the treatment of PBS solution.

Drug Loading and In Vitro Release. Briefly, 0.100 g of EGSA-NGs was weighed and dissolved in 50 mL of water. In addition, 0.080 g of berberine hydrochloride was placed in a test tube, and 5 mL of *N*,*N*-dimethylformamide (DMF) was added with ultrasonic assistance for the dissolution. The prepared berberine hydrochloride DMF solution was added dropwise to the EGSA-NG solution under stirring. After the completion of the dropwise addition, the mixture was stirred for 24 h and dialyzed against 2 L of distilled water for 48 h to remove the nonencapsulated berberine hydrochloride and residual DMF, and the solution outside the dialysis bag was retained as a standby test. The solution in the dialysis bag was freeze-dried to obtain berberine hydrochloride-loaded NGs.

Briefly, 0.2135 g of berberine hydrochloride was accurately weighed in a 1000 mL volumetric flask, brought to volume with distilled water, and ultrasonically dissolved at room temperature to prepare a berberine hydrochloride mother liquor. Subsequently, 1, 2, 3, 4, and 5 mL of berberine mother liquor were added into five 100 mL volumetric flasks, brought to volume with distilled water, and shaken evenly. The UV absorbance of berberine solution at each concentration was determined at a wavelength of 334 nm and recorded using a UV spectrophotometer to plot a standard curve of berberine hydrochloride.

The UV absorbance at 334 nm of test standby in the drug loading step was measured using a UV spectrophotometer. The concentration of berberine in the dialysate was calculated from the standard curve of berberine hydrochloride.

Phosphate buffer solution (pH = 7.4 or 5.5) and acetic acid buffer solution (pH = 4.5) were prepared, which corresponded to environmental pH of human blood or cytoplasmic streaming, environmental pH of the endosome in solid tumor cells, and environmental pH of the lysosome in solid tumor cells, respectively. Three batches of 0.010 g of berberine hydrochloride-loaded EGSA-NGs were dissolved in 3 mL of distilled water. Subsequently, the solutions were quickly transferred to 5000 Da dialysis bags, and the three sets of dialysis bags were separately immersed in 60 mL of three preformulated buffer solutions with different pH values. The in vitro drug release test was carried out at 37 °C in a water bath at a constant temperature. The release capacity of EGSA-NGs was tested within 24 h. After the buffer solution was taken out every 1, 2, 3, 4, 6, 8, 12, and 24 h, the same volume of buffer solution was added to continue dialysis.

The UV absorbance of the removed buffer solutions at a wavelength of 344 nm was determined using a UV

https://dx.doi.org/10.1021/acsomega.0c03965
ACS Omega 2021, 6, 1119−1128

spectrophotometer, the berberine concentration in the dialysate was calculated using the berberine hydrochloride standard curve, the cumulative release at the three pH values was calculated, and the cumulative release curve was plotted.

AUTHOR INFORMATION

Corresponding Authors

Dawei Qin − *School of Chemistry and Chemical Engineering, Qilu University of Technology (Shandong Academy of Sciences), Jinan 250353, China;* orcid.org/0000-0002-8525-598X; Email: daweiqin109@163.com

Mengli Zhang − *Qilu University of Technology Hospital, Qilu University of Technology (Shandong Academy of Sciences), Jinan 250353, China*; Email: 13791017381@126.com

Authors

Shuhua Chang − *School of Chemistry and Chemical Engineering, Qilu University of Technology (Shandong Academy of Sciences), Jinan 250353, China*

Rongjun Yan − *Jinan International Travel Health Care Center, Jinan 250353, China*

Binglin Sui − *School of Chemistry and Chemical Engineering, Qilu University of Technology (Shandong Academy of Sciences), Jinan 250353, China*

Hui Xu − *Qilu University of Technology Hospital, Qilu University of Technology (Shandong Academy of Sciences), Jinan 250353, China*

Zhaomin Zheng − *Qilu University of Technology Hospital, Qilu University of Technology (Shandong Academy of Sciences), Jinan 250353, China*

Xiaoli Hou − *Qilu University of Technology Hospital, Qilu University of Technology (Shandong Academy of Sciences), Jinan 250353, China*

Yonggang Wang − *Laboratory and Equipment Management, Qilu University of Technology (Shandong Academy of Sciences), Jinan 250353, China*

Chenggang Qi − *Laboratory and Equipment Management, Qilu University of Technology (Shandong Academy of Sciences), Jinan 250353, China*

Complete contact information is available at: https://pubs.acs.org/10.1021/acsomega.0c03965

Funding

The work was funded by the Shandong Provincial Natural Science Foundation of China (No. ZR2017LC005).

Notes

The authors declare no competing financial interest.

The data used to support the findings of this study are included within the article.

REFERENCES

(1) Hu, S.; Yi, T.; Huang, Z.; Liu, B.; Wang, J.; Yi, X.; Liu, J. Etching silver nanoparticles using DNA. *Mater. Horiz.* **2019**, *6*, 155.

(2) Dong, K.; Liu, Q.; Wei, G.; Hu, T.; Yao, J.; Zhang, X.; Gao, T. Mussel-inspired magnetic adsorbent: Adsorption/reduction treatment for the toxic Cr(VI) from simulated wastewater. *J. Appl. Polym. Sci.* **2018**, *135*, 46530.

(3) Zhang, X.; Li, Y.; Wei, M.; Liu, C.; Yu, T.; Yang, J. Cetuximab-modified silica nanoparticle loaded with ICG for tumor-targeted combinational therapy of breast cancer. *Drug Delivery* **2019**, *26*, 129.

(4) Zhang, C.-j.; Gao, Z.-y.; Wang, Q.-b.; Zhang, X.; Yao, J.-s.; Qiao, C.-d.; Liu, Q.-z. Highly Sensitive Detection of Melamine Based on the Fluorescence Resonance Energy Transfer between Conjugated Polymer Nanoparticles and Gold Nanoparticles. *Polymer* **2018**, *10*, 873.

(5) Maiti, D.; Chao, Y.; Dong, Z.; Yi, X.; He, J.; Liu, Z.; Yang, K. Development of a thermosensitive protein conjugated nanogel for enhanced radio-chemotherapy of cancer. *Nanoscale* **2018**, 13976.

(6) Liu, K.; Zheng, D.; Zhao, J.; Tao, Y.; Wang, Y.; He, J.; Lei, J.; Xi, X. pH-sensitive nanogels based on the electrostatic self-assembly of radionuclide ^{131}I labeled albumin and carboxymethyl cellulose for synergistic combined chemo-radioisotope therapy of cancer. *J. Mater. Chem. B* **2018**, 4738.

(7) Medeiros, S. F.; Santos, A. M.; Fessi, H.; Elaissari, A. Thermally-Sensitive and Magnetic Poly(N-Vinylcaprolactam)-Based Nanogels by Inverse Miniemulsion Polymerization. *J. Colloid Sci. Biotechnol.* **2012**, *1*, 99−112.

(8) Zan, M.; Li, J.; Huang, M.; Lin, S.; Luo, D.; Luo, S.; Ge, Z. Near-infrared light-triggered drug release nanogels for combined photo-thermal-chemotherapy of cancer. *Biomater. Sci.* **2015**, *3*, 1147−1156.

(9) Yu, S.; Hu, J.; Pan, X.; Yao, P.; Jiang, M. Stable and pH-sensitive nanogels prepared by self-assembly of chitosan and ovalbumin. *Langmuir* **2006**, *22*, 2754.

(10) Cheng, J.; Teply, B. A.; Sherifi, I.; Sung, J.; Luther, G.; Gu, F. X.; Levy-Nissenbaum, E.; Radovic-Moreno, A. F.; Langer, R.; Farokhzad, O. C. Formulation of functionalized PLGA−PEG nanoparticles for in vivo targeted drug delivery. *Biomaterials* **2007**, *28*, 869−876.

(11) Zucker, D.; Andriyanov, A. V.; Steiner, A.; Raviv, U.; Barenholz, Y. Characterization of PEGylated nanoliposomes co-remotely loaded with topotecan and vincristine: relating structure and pharmacokinetics to therapeutic efficacy. *J. Controlled Release* **2012**, *160*, 281−289.

(12) Momekova, D.; Momekov, G.; Lambov, N. NANO-SIZED DRUG DELIVERY PLATFORMS FOR TAXANE ANTINEOPLASTIC AGENTS. *FARMATSIJA* **2015**, *62*, 52−64.

(13) Miele, E.; Spinelli, G. P.; Miele, E.; Tomao, F.; Tomao, S. Albumin-bound formulation of paclitaxel (Abraxane® ABI-007) in the treatment of breast cancer. *Int. J. Nanomed.* **2009**, *4*, 99.

(14) Nakamoto, M.; Nonaka, T.; Shea, K. J.; Miura, Y.; Hoshino, Y. Design of synthetic polymer nanoparticles that facilitate resolubilization and refolding of aggregated positively charged lysozyme. *J. Am. Chem. Soc.* **2016**, *138*, 4282−4285.

(15) Torchilin, V. Tumor delivery of macromolecular drugs based on the EPR effect. *Adv. Drug Delivery Rev.* **2011**, *63*, 131−135.

(16) Tsukioka, Y.; Matsumura, Y.; Hamaguchi, T.; Koike, H.; Moriyasu, F.; Kakizoe, T. Pharmaceutical and biomedical differences between micellar doxorubicin (NK911) and liposomal doxorubicin (Doxil). *Jpn. J. Cancer Res.* **2002**, *93*, 1145−1153.

(17) Reynolds, C.; Barrera, D.; Jotte, R.; Spira, A. I.; Weissman, C.; Boehm, K. A.; Pritchard, S.; Asmar, L. Phase II trial of nanoparticle albumin-bound paclitaxel, carboplatin, and bevacizumab in first-line patients with advanced nonsquamous non-small cell lung cancer. *J. Thorac. Oncol.* **2009**, *4*, 1537−1543.

(18) Jain, R. K. Taming vessels to treat cancer. *Sci. Am.* **2008**, *298*, 56−63.

(19) Peng, P.-L.; Hsieh, Y.-S.; Wang, C.-J.; Hsu, J.-L.; Chou, F.-P. Inhibitory effect of berberine on the invasion of human lung cancer cells via decreased productions of urokinase-plasminogen activator and matrix metalloproteinase-2. *Toxicol. Appl. Pharmacol.* **2006**, *214*, 8−15.

(20) Wang, N.; Feng, Y.; Zhu, M.; Tsang, C.-M.; Man, K.; Tong, Y.; Tsao, S.-W. Berberine induces autophagic cell death and mitochondrial apoptosis in liver cancer cells: The cellular mechanism. *J. Cell. Biochem.* **2010**, *111*, 1426−1436.

(21) Fukuda, K.; Hibiya, Y.; Mutoh, M.; Koshiji, M.; Akao, S.; Fujiwara, H. Inhibition by berberine of cyclooxygenase-2 transcriptional activity in human colon cancer cells. *J. Ethnopharmacol.* **1999**, *66*, 227−233.

(22) Lü, Y.; Han, B.; Yu, H.; Cui, Z.; Li, Z.; Wang, J. Berberine regulates the microRNA-21-ITGB4-PDCD4 axis and inhibits colon cancer viability. *Oncol. Lett.* **2018**, *15*, 5971−5976.

(23) Grebinyk, A.; Yashchuk, V.; Bashmakova, N.; Gryn, D.; Hagemann, T.; Naumenko, A.; Kutsevol, N.; Dandekar, T.; Frohme, M. A new triple system DNA-Nanosilver-Berberine for cancer therapy. *Appl. Nanosci.* **2019**, *9*, 945−956.

https://dx.doi.org/10.1021/acsomega.0c03965
ACS Omega 2021, 6, 1119−1128